Geophys. J. R. astr. Soc. (1975) **40**, 465–474

On the Driving Forces of Plate Tectonics

J. F. Harper

(Received 1974 June 5)*

Summary

We suppose that the plates are pulled along on top of an effectively viscous asthenosphere by their cold dense sinking leading edges, and that they also tend to slide down the flanks of ocean ridge systems. Using reasonable literature values of density, viscosity and thickness, we find that a typical strong subduction zone pulls about seven times as hard as a typical mid-ocean ridge pushes. With the simplifying assumptions that other driving forces are much smaller, and the return current in the asthenosphere is everywhere (anti)parallel to the plate velocity, we perform a torque balance for each major plate in order to find its angular velocity, thus finding a set of relative angular velocities to compare with observations. The directions fit quite well but not the magnitudes. On the additional hypothesis that oceanic lithosphere thickens with age, owing to heat diffusion, the driving forces will be greater for large old plates. The fit is thereby greatly improved: predicted speeds are from 0·81 to 1·38 times the observed and the Cocos plate is not anomalous.

The model predicts tension in plates near their subduction zones. The Red Sea and African rift appear to have begun spreading as a crack moved into the former African + Arabian plate from a re-entrant corner off the Gulf of Aden which would have concentrated the stress. Gondwanaland may possibly have been split in a similar way.

Introduction

Two mechanisms which must help to drive plate motions are subduction-zone pull and mid-oceanic push (Orowan 1965; Elsasser 1969; Lliboutry 1969). There is considerable doubt whether they could be the principal mechanisms: see McKenzie (1969, 1972), Artyushkov (1973) and McKenzie, Roberts & Weiss (1974). We investigate the question by calculating the angular velocities which would result, for each plate in turn if no other driving forces acted, assuming that the motion is resisted only by Newtonian viscosity in the asthenosphere. Jeffreys (1970) gave a number of arguments against that last hypothesis, but they apply only when the total strain is small (10^{-2} or less). Continental drift involves strains of order 10 in the asthenosphere.

To estimate the force pulling a plate down at a subduction zone, let us suppose that the plate consists of rock $0{\cdot}05\,\mathrm{g\,cm^{-3}}$ heavier than the adjacent asthenosphere, in a 'tongue' 50 km thick which extends to a depth 300 km below the bottom of the horizontal part of the plate (Isacks & Molnar 1969, Hatherton 1970). Many plates go deeper, of course, but they then seem to be pushing into progressively stronger

---

* Received in original form 1973 December 18.

Table 1

Moments of forces on the various plates

(First approximation)

Plate and Locality	Type*	Length (deg)	Lat. (deg)	Long. (deg)	Azimuth (deg)	Moment/$5 \cdot 3 \times 10^{31}$ dyne cm		
						x	y	z
Antarctic Plate:								
S. Sandwich	C	5	−60	−25	−70	0·42	−0·46	0·33
Pacific Plate:								
California	C	15	30	−115	−50	−0·90	1·32	1·41
Alaskan Border	C	15	55	−135	−55	0·15	1·88	1·00
Aleutian	F+C	30	55	−165	30	−21·24	25·04	−9·82
W. Aleutian	C	5	55	165	−40	0·50	0·43	0·26
Kurile	F+C	20	50	155	50	−5·95	18·97	−11·25
Japan–Mariana	F+C	30	25	145	90	−11·87	8·31	−31·06
New Guinea	H+C	10	−5	140	180	−4·13	−4·92	0
New Brit.–New Hebr.	C	30	−10	160	150	−0·92	−3·60	−2·10
Tonga–NZ	F+C	30	−30	−175	65	14·21	15·78	−26·90
						−30·15	63·21	−78·46
Indian Plate:								
New Brit.–N. Hebr.	F1+C1	30	−10	160	−30	7·36	28·90	16·87
Burma–Indonesia	F1+C1	50	0	110	−40	41·12	14·97	36·72
Himalaya	C1	30	25	80	0	4·20	−0·74	0
						52·68	43·13	53·59
African Plate:								
Greece–Turkey	H+C	15	35	25	−15	2·63	−9·03	2·04
Mediterranean	C	30	40	0	0	0	−4·27	0
						2·63	−13·30	2·04
American Plate:								
Caribbean	H1	10	15	−65	135	3·59	0·66	−3·42
Mid-Arctic	M	15	87	90	−30	1·85	−1·07	0·06
Mid-Atlantic (15–75N)	M	60	45	−35	70	2·97	−5·65	−5·67
Mid-Atlantic(15N–2S)	M	40	7	−30	150	2·76	4.09	−2·82
Mid-Atlantic (2–55S)	M	55	−30	−5	100	−3·72	1·69	−6·67
S. Sandwich	H1	5	−60	−25	110	−1·48	1·64	−1·17
Scotia	M	20	−55	−50	0	−2·18	−1·83	0
						3·79	−0·47	−19·69
Eurasian Plate:								
Azores	M	5	40	−25	−15	−0·40	−0·58	0·14
Mid-Atlantic (40–75N)	M	35	57	−20	−105	−3·35	2·59	2·62
Mid-Arctic	M	15	87	90	150	−1·85	1·07	−0·06
						−5·60	3·08	2·70
Nazca Plate:								
Andes	F1+C1	52	−20	−73	−90	5·94	−19·43	55·82
Cocos Plate:								
Middle America	F+C	20	15	−93	−27	−20·18	3·74	10·02

* Types are as follows: C—compensating for mid-ocean ridges elsewhere (strength 0·142); F—full-strength subduction zone (strength 1·0); H—half-strength subduction zone (strength 0·5); M—mid-ocean ridge (strength 0·142). F1, C1, H1 denote moments which are halved in the second approximation, to allow for young thin lithosphere.

layers of the mantle rather than pulling on the upper parts of the plates (Isacks & Molnar 1969; Smith & Toksöz 1972). It is then easy to see that the horizontal component of the force acting on unit breadth of plate is $7{\cdot}5\times10^{15}$ dyne cm^{-1}, which is equivalent to a non-hydrostatic stress of 1500 bar in a slab 50 km thick. Many authors have found similar values, e.g. McKenzie (1969).

The pushing force per unit length of mid-ocean ridge is also easily estimated (Lliboutry 1969; Artyushkov 1974). An elevation of 2·5 km above the deep sea floor, density there $1{\cdot}6\ \mathrm{g\,cm^{-3}}$ higher than that of water, and an ultimate lithosphere thickness of 80 km give $1{\cdot}6\times10^{15}$ dyne cm^{-1} if the lithosphere is uniformly $0{\cdot}05\ \mathrm{g\,cm^{-3}}$ denser than the asthenosphere. On the more realistic hypothesis that the excess density varies linearly from zero at the bottom to $0{\cdot}1\ \mathrm{g\,cm^{-3}}$ at the top of the lithosphere, we obtain $1{\cdot}07\times10^{15}$ dyne cm^{-1}; this value will be adopted here. Because a uniform stress normal to its boundaries can cause no motion of a plate, it is equally valid when calculating the resultant moment about the centre of the Earth to use either a push of $1{\cdot}07\times10^{15}$ dyne cm^{-1} on those parts of the plate boundary which are mid-ocean ridges or a pull of the same magnitude on those which are not.

Several subduction zones appear to fade out at depths considerably less than 300 km. Wherever Barazangi & Dorman (1969) reported earthquakes between 100 and 200 km, but none deeper, we assign half the force per unit breadth of a 'full strength' subduction zone. In Table 1 we show the various zones and torque components adopted in this study. We use Cartesian axes with x towards latitude 0, longitude 0, y towards latitude 0, longitude +90° (i.e. 90° east), and z towards the North Pole (+90°), and assume a spherical Earth throughout. Units are chosen so that a 1° great-circle arc of full-strength subduction zone gives a moment of magnitude 1, half-strength magnitude 0·5, and of mid-ocean ridge 0·142. Azimuths indicate the direction of the force on the plate, measured from 0° (north) and increasing anticlockwise (i.e. +90° westwards). High accuracy was neither striven for nor, in view of the many approximations made in the theory, necessary.

Asthenospheric drag

To find a first approximation to the drag on a moving plate, we suppose that the plate, of thickness $h = 80$ km, overlies asthenosphere of thickness $\delta = 400$ km and Newtonian viscosity $\eta = 3{\cdot}1\times10^{20}$ poise (Christoffel & Calhaem 1973), and that the mantle below is so viscous that flow in it may be neglected. Values of both η and δ can be found in the literature which disagree with ours by large factors; as will be seen below, our results are sensitive only to the value of $\eta(4\delta+6h)/\delta^2$.

Curvature of the Earth will not seriously alter the parabolic velocity profile shown in Fig. 1 which results from assuming a plate velocity V throughout the depth h,

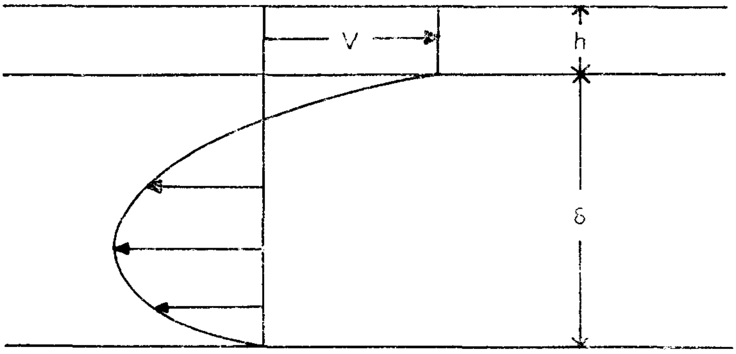

FIG. 1. Velocity profiles assumed in the lithosphere and asthenosphere.

and a return current in the asthenosphere, whose depth is small compared with the size of the plate. The drag force per unit area of plate is then $-\eta V(4\delta+6h)/\delta^2$. With the velocity vector equal to $\boldsymbol{\omega}\times\mathbf{r}$, where $\boldsymbol{\omega}$ is the angular velocity of a plate relative to the rigid deep mantle and $\mathbf{r}$ the radius vector from the centre of the Earth, we find that the resultant moment $\mathbf{M}$ of the forces driving the plate must be given by

$$\mathbf{M} = \frac{\eta(4\delta+6h)}{\delta^2}\iint \mathbf{r}\times(\boldsymbol{\omega}\times\mathbf{r})dA = \frac{\eta(4\delta+6h)}{\delta^2}I\boldsymbol{\omega}, \tag{1}$$

where the integral is over the area occupied by the plate, and I is the inertia tensor, referred to the Earth's centre as origin, of a thin lamina of unit surface density spread over the plate.

Results

Inertia tensors and their inverses were calculated for the eight plates considered by Chase (1972), i.e. Antarctic, Pacific, Indian, African, American, Eurasian, Nazca and Cocos. The Arabian, Caribbean and Philippine plates were excluded, the Scotia plate was included in the Antarctic, and other plate boundaries were taken from Chase (1972) and Barazangi & Dorman (1969). All integrations were done numerically on a grid at 10° intervals in both latitude and longitude, except for the small Cocos plate where 5° was used. The results are shown in Table 2, together with angular velocity components calculated from equation (1) and the moments in Table 1. The unit of moment of inertia used in Table 2 was chosen so that a 'square' 10° × 10° centred on the equator has unit moment about the polar axis. In the units of Tables 1 and 2, equation (1) gives $\boldsymbol{\omega} = 5{\cdot}399\ I^{-1}\mathbf{M}$.

Table 3 presents a comparison between the computed relative angular velocities and those of Chase (1972), for all plate pairs for which Chase had a reasonable number of measurements of both rate and direction. The agreement between computed and observed motions seems tolerable in view of the highly simplified model we used, except for the Cocos plate. Part of the trouble there arises because the plate is small, and so a small error in the positions of the forces acting on it causes a large error in the rate of rotation about its own centroid. In an attempt to counter this effect, equation (1) was used to find the resultant moment which was consistent with Chase's determination of the plate's motion relative to the Pacific and ours for the Pacific relative to the deep mantle. The result is that the Cocos plate would be driven in the proper direction at the proper rate by a torque with components ($-2{\cdot}89$, $0{\cdot}49$, $2{\cdot}21$) in the units of Table 1, i.e. with a magnitude 0·161 times that of Table 1 about an axis 11° away. The error in position seems acceptably small. It is consistent with a force crossing the subduction zone at latitude 13°, longitude $-90°$ in azimuth $-38°$, respectively 2°, 3° and 11° from the values given in Table 1.

The error in magnitude indicates a serious deficiency in the model, however. Part of it could arise from the small area of the plate: the velocity profile of Fig. 1 would not be fully developed near plate edges, and for the Cocos plate that means a large fraction of the area. But much of the error could arise from the plate's small thickness. The pull per unit breadth on a plate of thickness h propelled mainly by a subduction zone extending to depth d is proportional to hd, while the resisting force is proportional to LV, where L is the plate's length and V the velocity. So $L/t \propto V \propto hd/L \propto t^{\frac{1}{2}}d/L$, where t is the time required for a point on the plate to cross it, and we have used the proportionality $h \propto t^{\frac{1}{2}}$ which Turcotte & Oxburgh (1969) deduced from the theory of heat diffusion into the growing plate. Hence $h \propto L^{\frac{2}{3}}d^{-\frac{1}{3}}$, and the driving force per unit breadth $\propto L^{\frac{2}{3}}d^{\frac{2}{3}}$. L for the Cocos plate is about one-tenth that of the Pacific plate, while d has similar values, and so we would expect a driving force only $10^{-\frac{2}{3}} = 0{\cdot}217$ times as strong. This factor is not far from the 0·161 which would explain its observed speed.

Table 2

Plate inertia tensors, inverse tensors, and first and second approximations for the velocity components

Plate	Inertia tensor	Inverse tensor	Angular velocity ($\times 10^{-7}$ deg/yr)	
Antarctic	$\begin{pmatrix} 45{\cdot}3 & -1{\cdot}6 & 2{\cdot}1 \\ -1{\cdot}6 & 39{\cdot}6 & 2{\cdot}4 \\ 2{\cdot}1 & 2{\cdot}4 & 13{\cdot}2 \end{pmatrix}$	$\begin{pmatrix} 0{\cdot}0223 & 0{\cdot}0011 & -0{\cdot}0038 \\ 0{\cdot}0011 & 0{\cdot}0256 & -0{\cdot}0049 \\ -0{\cdot}0038 & -0{\cdot}0049 & 0{\cdot}0771 \end{pmatrix}$	$\begin{pmatrix} 0{\cdot}039 \\ -0{\cdot}069 \\ 0{\cdot}142 \end{pmatrix}$	$\begin{pmatrix} \text{no} \\ \text{change} \end{pmatrix}$
Pacific	$\begin{pmatrix} 40{\cdot}5 & -13{\cdot}0 & 2{\cdot}4 \\ -13{\cdot}0 & 67{\cdot}9 & -1{\cdot}7 \\ 2{\cdot}4 & -1{\cdot}7 & 69{\cdot}6 \end{pmatrix}$	$\begin{pmatrix} 0{\cdot}0263 & 0{\cdot}0050 & -0{\cdot}0008 \\ 0{\cdot}0050 & 0{\cdot}0157 & 0{\cdot}0002 \\ -0{\cdot}0008 & 0{\cdot}0002 & 0{\cdot}0144 \end{pmatrix}$	$\begin{pmatrix} -2{\cdot}236 \\ 4{\cdot}460 \\ -6{\cdot}161 \end{pmatrix}$	$\begin{pmatrix} \text{no} \\ \text{change} \end{pmatrix}$
Indian	$\begin{pmatrix} 37{\cdot}1 & 5{\cdot}2 & -7{\cdot}4 \\ 5{\cdot}2 & 21{\cdot}7 & 7{\cdot}7 \\ -7{\cdot}4 & 7{\cdot}7 & 41{\cdot}1 \end{pmatrix}$	$\begin{pmatrix} 0{\cdot}0298 & -0{\cdot}0098 & 0{\cdot}0072 \\ -0{\cdot}0098 & 0{\cdot}0526 & -0{\cdot}0117 \\ 0{\cdot}0072 & -0{\cdot}0117 & 0{\cdot}0279 \end{pmatrix}$	$\begin{pmatrix} 8{\cdot}277 \\ 6{\cdot}075 \\ 7{\cdot}396 \end{pmatrix}$	$\begin{pmatrix} 4{\cdot}138 \\ 3{\cdot}038 \\ 3{\cdot}698 \end{pmatrix}$
African	$\begin{pmatrix} 20{\cdot}0 & -7{\cdot}3 & 2{\cdot}0 \\ -7{\cdot}3 & 49{\cdot}9 & 3{\cdot}3 \\ 2{\cdot}0 & 3{\cdot}3 & 52{\cdot}7 \end{pmatrix}$	$\begin{pmatrix} 0{\cdot}0532 & 0{\cdot}0079 & -0{\cdot}0026 \\ 0{\cdot}0079 & 0{\cdot}0213 & -0{\cdot}0017 \\ -0{\cdot}0026 & -0{\cdot}0017 & 0{\cdot}0192 \end{pmatrix}$	$\begin{pmatrix} 0{\cdot}159 \\ -1{\cdot}436 \\ 0{\cdot}297 \end{pmatrix}$	$\begin{pmatrix} \text{no} \\ \text{change} \end{pmatrix}$
American	$\begin{pmatrix} 60{\cdot}2 & 13{\cdot}3 & 6{\cdot}5 \\ 13{\cdot}3 & 49{\cdot}1 & 7{\cdot}3 \\ 6{\cdot}5 & 7{\cdot}3 & 44{\cdot}9 \end{pmatrix}$	$\begin{pmatrix} 0{\cdot}0178 & -0{\cdot}0045 & -0{\cdot}0018 \\ -0{\cdot}0045 & 0{\cdot}0220 & -0{\cdot}0029 \\ -0{\cdot}0018 & -0{\cdot}0029 & 0{\cdot}0230 \end{pmatrix}$	$\begin{pmatrix} 0{\cdot}567 \\ 0{\cdot}160 \\ -2{\cdot}475 \end{pmatrix}$	$\begin{pmatrix} 0{\cdot}468 \\ 0{\cdot}219 \\ -2{\cdot}264 \end{pmatrix}$
Eurasian	$\begin{pmatrix} 47{\cdot}3 & 3{\cdot}0 & -5{\cdot}3 \\ 3{\cdot}0 & 38{\cdot}1 & -14{\cdot}0 \\ -5{\cdot}3 & -14{\cdot}0 & 28{\cdot}7 \end{pmatrix}$	$\begin{pmatrix} 0{\cdot}0216 & -0{\cdot}0003 & 0{\cdot}0039 \\ -0{\cdot}0003 & 0{\cdot}0319 & 0{\cdot}0155 \\ 0{\cdot}0039 & 0{\cdot}0155 & 0{\cdot}0431 \end{pmatrix}$	$\begin{pmatrix} -0{\cdot}602 \\ 0{\cdot}765 \\ 0{\cdot}768 \end{pmatrix}$	$\begin{pmatrix} \text{no} \\ \text{change} \end{pmatrix}$
Nazca	$\begin{pmatrix} 14{\cdot}4 & -0{\cdot}1 & -0{\cdot}1 \\ -0{\cdot}1 & 2{\cdot}3 & -3{\cdot}8 \\ -0{\cdot}1 & -3{\cdot}8 & 13{\cdot}1 \end{pmatrix}$	$\begin{pmatrix} 0{\cdot}0696 & 0{\cdot}0087 & 0{\cdot}0029 \\ 0{\cdot}0087 & 0{\cdot}8307 & 0{\cdot}2419 \\ 0{\cdot}0029 & 0{\cdot}2419 & 0{\cdot}1470 \end{pmatrix}$	$\begin{pmatrix} 2{\cdot}19 \\ -13{\cdot}96 \\ 19{\cdot}02 \end{pmatrix}$	$\begin{pmatrix} 1{\cdot}097 \\ -6{\cdot}981 \\ 9{\cdot}509 \end{pmatrix}$
Cocos	$\begin{pmatrix} 2{\cdot}19 & -0{\cdot}16 & 0{\cdot}03 \\ -0{\cdot}16 & 0{\cdot}09 & 0{\cdot}33 \\ 0{\cdot}03 & 0{\cdot}33 & 2{\cdot}16 \end{pmatrix}$	$\begin{pmatrix} 0{\cdot}67 & 2{\cdot}78 & -0{\cdot}44 \\ 2{\cdot}78 & 36{\cdot}53 & -5{\cdot}65 \\ -0{\cdot}44 & -5{\cdot}65 & 1{\cdot}34 \end{pmatrix}$	$\begin{pmatrix} -40{\cdot}32 \\ 129{\cdot}32 \\ 5{\cdot}87 \end{pmatrix}$	$\begin{pmatrix} \text{see} \\ \text{text} \end{pmatrix}$

Table 3

Comparison of observed and computed relative angular velocities of plates. Latitudes and longitudes are of the poles of rotation, in degrees. Rates are in units of 10^{-7} *deg/yr. Distances are between computed and observed positions, in degrees. Speed factors are computed rates divided by observed.*

Plate pair		Lat.	Long.	Rate	Dist.	Speed factor
Pac–Ant	Observed	−70	107	9·76		
	1st approx.	−51	117	8·09	20	0·83
Ind–Ant	Observed	16	24	6·50		
	1st approx.	35	36	12·63	22	1·94
	2nd approx.	35	37	6·25	22	0·96
Ame–Pac	Observed	52	−73	7·86		
	1st approx.	36	−57	6·32	20	0·80
	2nd approx.	37	−57	6·36	18	0·81
Afr–Ame	Observed	66	−29	3·44		
	1st approx.	59	−104	3·22	33	0·94
	2nd approx.	57	−101	3·06	33	0·89
Ind–Afr	Observed	15	48	6·33		
	1st approx.	33	43	13·19	19	2·08
	2nd approx.	30	48	6·89	15	1·09
Eua–Ame	Observed	48	155	2·36		
	1st approx.	68	153	3·50	20	1·48
	2nd approx.	68	153	3·26	20	1·38
Naz–Pac	Observed	59	−97	14·6		
	1st approx.	53	−72	31·7	15	2·17
	2nd approx.	53	−73	19·7	15	1·35
Coc–Naz	Observed	8	−116	11·9		
	1st approx.	−5	107	105	138	8·8
	2nd approx.	(see text)			11	1·35

By the same argument, the subduction-zone pull on the American plate, and all the torques on the Indian and Nazca plates, should be reduced by nearly half. The second approximation presented in Tables 2 and 3 was computed using a factor of exactly one-half. Its effect is to reduce all the large discrepancies between calculated and observed plate speeds, so that their ratios now range from 0·81 to 1·38 (instead of 0·80 to 8·8 as in the first approximation).

This improved fit requires the $t^{\frac{1}{2}}$ dependence of thickness to continue for over 100 My. It is usually held that Sclater, Anderson & Bell (1971) proved the contrary, but the sea is a few hundred metres deeper than their theory predicts above both very young and very old oceanic crust, and shallower for intermediate ages. Our asthenospheric flow pattern (Fig. 1) implies that the pressure is higher under the leading end of each plate than the trailing end, which deepens the sea near mid-ocean ridges and makes it shallower near trenches, by some hundreds of metres. Fig. 2 of Sclater *et al.* shows the effect clearly for crust younger than 40 My, and would show it also for older crust if the $t^{\frac{1}{2}}$ dependence were continued.

Plate splitting

So far, we have taken plate boundaries and subduction zones where we find them. Can we do more? A simple explanation can be suggested at least for the Red Sea and African rift valley. Before these opened up, the Arabian plate was part of the African

FIG. 2. The African and Arabian plates. Spreading ridges and transform faults are indicated schematically by dotted lines, compressional boundaries by continuous lines, and active subduction zones by arrows.

plate, with an active subduction zone under the Zagros mountains and eastern Mediterranean. There would therefore have been quite large forces pulling the plate in the general direction of the arrows in Fig. 2. Close by, there was a re-entrant corner at A on the boundary with the Indian plate, which would magnify the stresses locally, presumably enough to start a crack. This crack then began to propagate towards B, where it bifurcated into BD going up the future Red Sea and BC down the African rift. Both branches have bifurcated again at corners, but the particular courses they follow must depend on the local geology. The crack AB has since moved slightly north of the sharp corner because the Arabian plate has been moving north faster than the Indian (McKenzie & Sclater 1971).

Since Arabia split off, the African plate has had only one small subduction zone. Presumably this is why the crack BC has not reached the African–Antarctic boundary. The net force on the plate is still northward (Table 1), as is the motion (Table 2), and so the Somali plate fragment east of the rift is being pushed from behind, at one side. This may account for its present small clockwise rotation relative to Africa. (Treating it as a separate plate by the methods used for Tables 1 and 2 improves the African–American angular velocity misfit but does not yield sensible results for the Somali plate itself: the model does not yet include interactions between plates of the kind which must occur here.)

Some other plate boundaries could have started in the same way at re-entrant corners concentrating a tensile horizontal deviatoric stress. The reconstructions of Dietz & Holden (1.70) show many propagating cracks, mostly in regions where a subduction zone would help to open them, but their only good example of a re-entrant corner is in the Jurassic Caribbean sea. This would readily explain a crack going south between Africa and South America, but it actually seems to have gone the other way. If we accept Smith & Hallam's (1970) map of Gondwanaland, though, and assume that the first crack went between Antarctica and Africa–India, it may have turned sharply around the Antarctic Peninsula. Re-entrant corners would then have been available to start the splits between South America and Africa and between Australia and Antarctica.

Discussion

In the present state of knowledge one can speculate about the origin of plates almost at will. The real justification for our model is the way it accounts for the present velocities of plates varying in size from the Cocos to the Pacific, and covering most of the Earth's surface. Some problems do remain, though. The largest plates not so far considered are the Arabian and Philippine. Both are small enough to require a treatment like the Cocos, where observed velocities are used to find torques, because the reverse process would lead to ill-conditioned equations. The Arabian plate is presumably still being pulled away from Africa by the shallow Zagros slab, aided by ' midoceanic push ' in the Red Sea, but detailed calculation must await a better determination of the African plate's velocity relative to the deep mantle. Table 3, and the discussion of the African rift in the previous section, make one suspect that there are still significant errors. As for the Philippine plate, all one can say in the absence of speed measurements is that the Ryukyu and Philippine trenches are pulling it in something like the expected direction.

The theory does not explain the motion of such plates as the Caribbean, which have no subduction zones of their own but are pulled by such zones belonging to other plates. McKenzie (1969) has shown how to calculate the forces involved. As they are small compared with those considered here, one would expect the Caribbean plate to be moving slowly, which it is, and that only very small plates like the Turkish could be moved at rates comparable to the major plates by this means, or by direct pushing from adjacent plates. Our model of plate motions also does not explain why the Eurasian plate behaves so differently from the American above a subduction zone: the Eurasian has a large number of fragments, while the American has two at most (the Caribbean and Scotia seas).

An objection which might be raised to our model is that the tension near the oceanic side of a sinking slab would tear the plate apart and prevent forces being transmitted to the remainder. Normal faults do indeed occur there, but hydrostatic pressure must make all the principal stresses compressive below a few kilometres, and this allows the lithosphere to act as a ' stress guide ' to the remainder of the plate (Elsasser 1969).

McKenzie *et al.* (1974) have offered another objection that ' if the temperature difference between the sinking slab of thickness 70 km and the mantle is 1000 °C, then the temperature difference across regions 5000 km in extent must be much less than 15 °C if the buoyancy force of the boundary layer is to dominate '. If that argument were valid, it would also show that the mid-ocean push on a plate was vastly greater than the subduction zone pull. McKenzie *et al.* themselves point out that it is smaller.

Resistance caused by friction between the overthrusting and underthrusting plates where they are in contact at a subduction zone has been neglected in this study. It would be more important for the thinner plates; according to Table 3 their velocities are still in need of reduction.

Conclusions

It is possible to account for the major part of the motion of the eight principal plates without considering any driving forces except the well-known downward pull at subduction zones and outward push from mid-ocean ridges, and with the simplest possible hypothesis for flow in the asthenosphere. As some of the numerical parameters on which the theory depends are poorly known, this could be coincidental, and the actual driving forces could be quite different. The actual resistance to strain in the asthenosphere could likewise be governed by non-Newtonian laws of viscosity. But the model chosen here seems reasonable and does explain most of the facts. It also explains the location of the one plate boundary at present forming far from any old boundary—the African rift. It may also help to explain how Gondwanaland split apart.

After this work was submitted for publication, an independent analysis of the same problem appeared, by Solomon & Sleep (1974). They consider a greater variety of resistances to motion, but take all relative velocities as given instead of trying to predict them. Their results for absolute velocities relative to the deep mantle are very insensitive to the particular drag mechanism assumed. Our relative plate velocities are, on the other hand, sensitive enough to provide a useful means of testing the theories, and further work in this direction is in progress.

Acknowledgments

Many helpful comments and suggestions were made by J. H. Ansell, I. Calhaem, D. A. Christoffel, R. K. H. Falconer, T. Hatherton, E. G. C. Smith and a referee. Computing facilities were provided by the Applied Mathematics Division, N.Z. Department of Scientific and Industrial Research.

Department of Mathematics and Institute of Geophysics,
Victoria University of Wellington,
Wellington, New Zealand.

References

Artyushkov, E. V., 1973. Stresses in the lithosphere caused by crustal thickness inhomogeneities, *J. geophys. Res.*, **78**, 7675–7708.

Artyushkov, E. V., 1974. Can the Earth's crust be in a state of isostasy? *J. geophys. Res.*, **79**, 741–752.

Barazangi, M. & Dorman, J., 1969. World seismicity maps compiled from ESSA, Coast and Geodetic Survey, Epicenter data, 1961–67, *Bull. seism. Soc. Am.*, **59**, 369–380.

Chase, C. G., 1972. The N plate problem of plate tectonics, *Geophys. J. R. astr. Soc.*, **29**, 117–122.

Christoffel, D. A. & Calhaem, I., 1973. Upper mantle viscosity determined from Stokes's law, *Nature*, **243**, 51–52.

Dietz, R. G. & Holden, J. C., 1970. The breakup of Pangaea, *Scientific American*, **223** (4), 30–41.

Elsasser, W. M., 1969. Convection and stress propagation in the upper mantle, *The application of modern physics to the Earth and planetary interiors*, pp. 223–246, ed. S. K. Runcorn, Wiley–Interscience, New York.

Hatherton, T., 1970. Upper mantle inhomogeneity beneath New Zealand: surface manifestations, *J. geophys. Res.*, **75**, 269–284.

Isacks, B. & Molnar, P., 1969. Mantle earthquake mechanisms and the sinking of the lithosphere, *Nature*, **223**, 1121–1124.

Jeffreys, H., 1970. Imperfections of elasticity and continental drift, *Nature*, **225,** 1007–1008.

Lliboutry, L., 1969. Sea floor spreading, continental drift and lithosphere sinking with an asthenosphere at melting point, *J. geophys. Res.*, **74,** 6525–6540.

McKenzie, D. P., 1969. Speculations on the causes and consequences of plate motions, *Geophys. J. R. astr. Soc.*, **18,** 1–32.

McKenzie, D. P., 1972. Plate tectonics, *The nature of the solid Earth*, pp. 323–360, ed. E. C. Robertson, McGraw-Hill, New York.

McKenzie, D. P. & Sclater, J. G., 1971. The evolution of the Indian Ocean since the late Cretaceous, *Geophys. J. R. astr. Soc.*, **24,** 437–528.

McKenzie, D. P., Roberts, J. M. & Weiss, N. O., 1974. Convection in the Earth's mantle: towards a numerical simulation, *J. fluid Mech.*, **62,** 465–538.

Orowan, E., 1965. Convection in a non-Newtonian mantle, continental drift, and mountain building, *Phil. Trans. R. Soc. Lond.*, **A258,** 284–313.

Sclater, J. G., Anderson, R. N. & Bell, M. L., 1971. Elevation of ridges and evolution of the central eastern Pacific, *J. geophys. Res.*, **76,** 7888–7915.

Smith, A. G. & Hallam, A., 1970. The fit of the southern continents, *Nature*, **225,** 139–144.

Smith, A. T. & Toksöz, M. N., 1972. Stress distribution beneath island arcs, *Geophys. J. R. astr. Soc.*, **29,** 289–318.

Solomon, S. C. & Sleep, N. H., 1974. Some simple physical models for absolute plate motions, *J. geophys. Res.*, **79,** 2557–2567.

Turcotte, D. L. & Oxburgh, E. R., 1969. Convection in a mantle with variable physical properties, *J. geophys. Res.*, **74,** 1458–1474.